



# Synthesis of glycerol carbonate by transesterification of glycerol with dimethyl carbonate over MgAl mixed oxide catalysts



Peng Liu<sup>a,\*</sup>, Margherita Derchi<sup>b</sup>, Emiel J.M. Hensen<sup>a,\*</sup>

<sup>a</sup> Department of Chemical Engineering and Chemistry, Eindhoven University of Technology, P.O. Box 513, Eindhoven, The Netherlands

<sup>b</sup> Dipartimento di Ingegneria Chimica, Civile e Ambientale, Università degli Studi di Genova, I-16145 Genova, Italy

## ARTICLE INFO

### Article history:

Received 20 April 2013

Received in revised form 23 June 2013

Accepted 3 July 2013

Available online 19 July 2013

### Keywords:

Heterogeneous catalysis

Transesterification

Hydrotalcite

Layered double hydroxides

Glycerol carbonate

## ABSTRACT

A series of hydrotalcite-like layered double hydroxides (LDHx) with different Mg/Al atomic ratios ( $x = 2-6$ ) were prepared by using the co-precipitation method. Further calcination yields mixed oxides with tunable basicity. The basicity of the calcined LDHx (LDOx) strongly depends on the Mg/Al ratio and the calcination temperature. The resulting LDOx materials were used as solid base catalysts and evaluated in the transesterification between glycerol and dimethyl carbonate without use of organic solvent. The correlation between the basic properties of the solid catalysts and the catalytic performance was investigated. The activity of the LDOx catalysts was demonstrated to be proportional to the surface density of basic sites. LDO2 calcined at 600 °C exhibited maximum activity for the transesterification reaction. The beneficial effect of the optimum ratio of Mg/Al = 2 is related to its high total basicity. The LDO2 catalyst can be readily recycled while maintaining high catalytic activity and selectivity of glycerol carbonate.

© 2013 Elsevier B.V. All rights reserved.

## 1. Introduction

Since the demand for biomass-derived biofuels is increasing globally, the utilization of surplus byproduct glycerol as a platform chemical represents a promising opportunity to obtain value-added products from renewable raw materials [1–3]. Glycerol carbonate (GLC) is one of the glycerol derivatives that attracts significant scientific and industrial interest due to its low toxicity, low flammability, biodegradability and high boiling point [4,5]. GLC has found applications as a high boiling polar solvent, an intermediate in organic synthesis and in the synthesis of polycarbonates, polyurethanes, glycidol-based polymers and surfactants [5]. The direct carbonylation of glycerol with CO<sub>2</sub> to GLC, involving two abundant waste streams, is the most desirable route to replace the traditional reaction of glycerol with harmful phosgene. Attempts have been made to use homogeneous tin complexes, however, the unfavorable thermodynamic equilibrium and low yields limit the applicability of such processes [6,7]. The direct reaction of glycerol with supercritical CO<sub>2</sub> was also attempted using zeolites as catalysts [8], but there is no evidence that direct CO<sub>2</sub> insertion occurred as GLC was only produced when another organic carbonate was added as a reactant. The alternative routes include the carbonylation of glycerol with urea and the transesterification

of glycerol with alkyl carbonates. Although carbonylation with urea has been described by using homogeneous inorganic salts, solid oxides and supported nanoparticles as catalysts, this reaction must be performed at high temperature (>120 °C) and low pressure (30–50 mbar) or under dry inert gas flow to shift the equilibrium toward GLC formation by isolating produced ammonia continuously from the gaseous phase [9–12]. A more attractive route for industrial application would be transesterification between glycerol and alkyl carbonates, such as dimethyl carbonate (DMC) and diethyl carbonate (DEC), because of the milder and greener process conditions [4]. Base catalysis seems more promising than acid catalysis for this transesterification reaction, because higher conversion can be achieved by using basic catalysts [13]. Regarding base catalysis solid bases are in particular interesting due to the fact that corrosion problem and waste formation can be avoided and, furthermore, solid catalysts can be easily recovered and reused [14,15].

Among the wide range of solid bases, hydrotalcite (Mg<sub>6</sub>Al<sub>2</sub>(OH)<sub>16</sub>CO<sub>3</sub>·nH<sub>2</sub>O) type layered double hydroxides (LDH) attract significant industrial interest [16,17] and are the subject of many academic investigation [18]. Being basic in nature, LDHs have been widely studied for various base-catalyzed or -assisted reactions such as alkylation, Michael addition, Claisen-Schmidt condensation, Knoevenagel condensation, aldol condensation, transesterification, hydrogenation, olefin epoxidation and alcohol oxidation [19–26]. Through controlled thermal decomposition, LDHs are converted to mixed oxides (LDO) with high specific surface areas, homogeneous dispersion of metal cations and

\* Corresponding authors. Tel.: +31 40 247 2833; fax: +31 40 245 5054.

E-mail addresses: [pliu503@hotmail.com](mailto:pliu503@hotmail.com), [p.liu@tue.nl](mailto:p.liu@tue.nl) (P. Liu), [e.j.m.hensen@tue.nl](mailto:e.j.m.hensen@tue.nl) (E.J.M. Hensen).

strong Lewis basic sites [27,28]. The basic properties of the LDO depend on the composition of metal cations in the precursor LDH. Interestingly, the catalytic activity of LDO can also be enhanced by rehydration in an inert atmosphere, which results in reconstruction of the original layered structure, with Brønsted basic sites  $\text{OH}^-$  as the charge compensating anions in the interlayer [29,30]. Consequently, the facile adjustment of the type of basic sites and surface base strength makes LDH versatile precursors for optimal solid base catalysts for a wide range of base-catalyzed reactions.

Recently, LDH-based solid base catalysts have shown promise for transesterification of glycerol to value-added GLC [31–38]. Uncalcined MgAl LDHs with co-existent hydromagnesite phase were found to be active catalysts for GLC synthesis from glycerol and DMC [31,32], but a larger amount of catalyst (~50 wt%) and a harmful solvent (*N,N*-dimethyl formamide) are needed for this reaction. Medina and co-workers reported that rehydrated MgAl LDH showed higher activity than the calcined MgAl LDO for transesterification of glycerol with DEC [33–35], but the active reconstructed LDH catalysts often deactivate rapidly due to the instability of surface Brønsted basic sites. Carbon nanofiber supported MgAl LDH, however, exhibited a different activity trend with calcined LDO showing higher activity than the rehydrated samples, although the calcined catalyst also deactivated upon reuse and showed lower GLC selectivity (<90%) [36]. Zr-doping MgAl LDH (Mg/Al/Zr = 3/1/1) showed optimal GLC yield when calcined at 650 °C, but without evidence on catalyst stability [37]. Although useful MgAl LDH-based catalysts were reported, to the best of our knowledge the effects of Mg/Al atomic ratio on the basicity of calcined  $\text{Mg}_x\text{Al}$  LDH (LDO $_x$ ) and their catalytic performance in the transesterification of glycerol with DMC to GLC remain unknown [34]. It remains a challenging task to develop more efficient and reusable catalysts for synthesis of GLC under mild and solvent-free conditions.

We have recently reported on the facile adjustment of the basicity of MgAl LDH by variation of the Mg/Al atomic ratio to render optimum  $\text{Mg}_x\text{Al}$  LDH supported gold nanoparticle catalysts for one-pot tandem reactions [26]. The basicity of the  $\text{Mg}_x\text{Al}$  LDH supports varied with the Mg/Al ratio ( $x = 2, 3, 4, 5, 6$ ), which tunes the alcohol dehydrogenation activity. Herein, we will show that the LDO $_x$  samples obtained by calcination of the  $\text{Mg}_x\text{Al}$  LDH precursors are efficient solid base catalysts for GLC synthesis from glycerol and DMC with GLC selectivity up to 100% under moderate (100 °C) and solvent-free conditions. Their activity can be tailored by simple adjustment of the calcination temperature. The correlations between the textural, chemical structures and the basic properties of the LDO $_x$  catalysts and the catalytic performance in the glycerol transesterification were investigated. Moreover, the optimal catalyst and reaction conditions were also determined.

## 2. Experimental

### 2.1. Catalyst preparation

A series of  $\text{Mg}_x\text{Al}$  LDH ( $x = 2, 3, 4, 5$  and 6) precursors were prepared by co-precipitation method as follows. Appropriate amounts of  $\text{Mg}(\text{NO}_3)_2 \cdot 6\text{H}_2\text{O}$  (20–60 mmol) and  $\text{Al}(\text{NO}_3)_3 \cdot 9\text{H}_2\text{O}$  (10 mmol) were dissolved in 100 mL of deionized water and added into a three-necked glass flask (500 mL) which initially contained  $\text{Na}_2\text{CO}_3$  (20 mmol) in 200 mL of deionized water. The pH was controlled by adding a 2 M NaOH solution and kept at  $10.0 \pm 0.5$ . Both solutions were added dropwise under vigorous stirring. The slurry was stirred overnight at room temperature, then the precipitate was filtered and washed intensively until neutral filtrate. The solid was dried at 110 °C overnight to yield the LDH $_x$  precursors, which were further calcined at 500 °C in air for 6 h to yield the LDO $_x$  catalysts.

### 2.2. Catalyst characterization

XRD was performed on a Bruker Endeavour D4 with  $\text{Cu K}\alpha$  radiation (40 kV and 30 mA). The BET surface areas were recorded on a Tristar 3000 automated gas adsorption system. The samples were degassed at 180 °C for 3 h prior to analysis. The metal composition of the LDH $_x$  was determined by ICP-OES after an aliquot of the sample was dissolved in  $\text{HNO}_3$ . Magic-angle spinning (MAS)  $^{27}\text{Al}$  NMR spectra were recorded on a Bruker DMX500 spectrometer equipped with a 4-mm MAS probe head operating at an Al NMR frequency of 130 MHz. The  $^{27}\text{Al}$  chemical shift is referenced to a saturated  $\text{Al}(\text{NO}_3)_3$  solution. In a typical experiment sample (10 mg) was packed in a 2.5 mm zirconia rotor. The MAS sample rotation speed was 25 kHz. The relaxation time was 1 s and the pulse length was 1  $\mu\text{s}$ .

X-ray photoelectron spectroscopy (XPS) measurements were performed using a Thermo Scientific K-Alpha spectrometer, equipped with a monochromatic small-spot X-ray source and a 180° double focusing hemispherical analyzer with a 128-channel detector. Spectra were obtained using an aluminum anode (Al  $\text{K}\alpha = 1486.6$  eV) operating at 72 W and a spot size of 400  $\mu\text{m}$ . Survey scans were measured at a constant pass energy of 200 eV and region scans at 50 eV. The background pressure was  $2 \times 10^{-9}$  mbar and during measurement  $3 \times 10^{-7}$  mbar Argon because of the charge compensation dual beam source. Data analysis was performed using CasaXPS software. The binding energy was corrected for surface charging by taking the C 1s peak of contaminant carbon as a reference at 284.5 eV.

Temperature programmed desorption of  $\text{CO}_2$  ( $\text{CO}_2$ -TPD) experiments were carried out for the measurement of basicity of the catalysts. After the catalyst (50 mg) was pre-treated at 500 °C for 1 h under He stream (50 mL/min), it was cooled down to 90 °C and  $\text{CO}_2$  (10 vol%) was introduced for adsorption at this temperature for 0.5 h. After the catalyst was swept with He for 60 min to remove the physisorbed  $\text{CO}_2$  from catalyst surface, the temperature was increased linearly with rate of 10 °C/min in He and the signal of  $\text{CO}_2$  ( $M/e = 44$ ) was recorded by online mass spectrometry (quadrupole mass spectrometer, Balzers TPG-300). The amount of  $\text{CO}_2$  was quantified by a calibration curve, which was established by thermal decomposition of known amounts of  $\text{NaHCO}_3$ .

Temperature programmed surface reactions (TPSR) of pre-adsorbed isopropanol were carried out as follows: after the LDO $_x$  catalyst (50 mg) was pre-treated at 500 °C for 1 h under He stream (50 mL/min), it was cooled to room temperature and isopropanol vapor was introduced for adsorption at room temperature for 0.5 h. After the catalyst was swept with He for 60 min, the temperature was increased linearly with rate of 10 °C/min in He and the signals of  $\text{H}_2$  ( $M/e = 2$ ), acetone ( $M/e = 43$  and  $M/e = 58$ ), and propene ( $M/e = 41$ ) were recorded by online mass spectrometry (quadrupole mass spectrometer, Balzers TPG-300) simultaneously.

### 2.3. Catalytic activity measurements

The transesterification of dimethyl carbonate and glycerol to glycerol carbonate was carried out using a 10 mL glass tube reactor with a reflux condenser. Typically, the reactor was charged with 5 mmol of glycerol, 15 mmol of dimethyl carbonate, 2 mmol of 1,4-butanediol (internal standard), and 10 wt% of catalyst (46 mg). The resulting mixture was stirred at 100 °C for 2 h then 5 mL of ethanol was added to quench the reaction. The used catalyst was separated by centrifugation, washed with ethanol and dried at 200 °C. Recovered catalyst can be reused in the next run under the same conditions. The reaction products were quantitatively analyzed by a Shimadzu QP5050 GC-MS (Stabilwax column, 30 m  $\times$  0.32 mm,  $d_f = 0.5$   $\mu\text{m}$ ) using an internal standard technique.

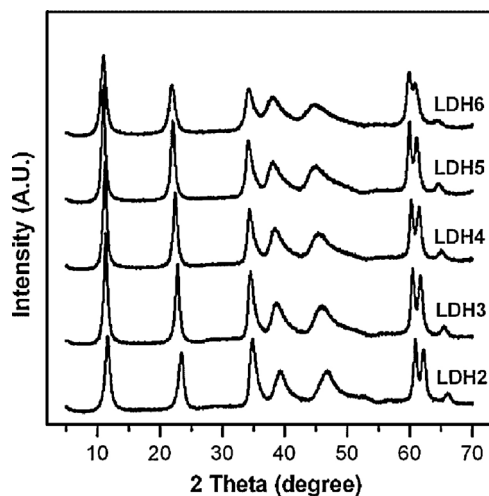


Fig. 1. XRD patterns of the LDHx precursors.

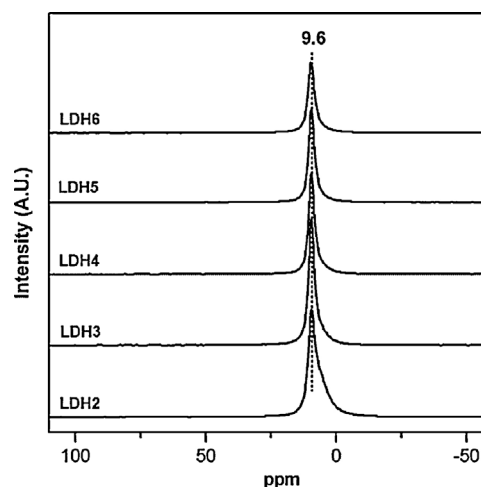


Fig. 2.  $^{27}\text{Al}$  MAS NMR spectra of the LDHx precursors.

### 3. Results and discussion

#### 3.1. Catalyst preparation and characterization

To study the influence of the “coprecipitation–calcination” process on the structural and chemical properties of the LDHx precursors and LDOx catalysts, various physico-chemical characterization techniques such as XRD,  $\text{N}_2$  physisorption, ICP-OES,  $^{27}\text{Al}$  MAS NMR and XPS were employed. Fig. 1 shows the XRD patterns of the LDHx precursors. All patterns contain the characteristic peaks corresponding to a well-defined hydrotalcite structure [16], although the peak intensities were somewhat decreased with the Mg/Al ratio increasing. This result indicates that by the coprecipitation method the Mg and Al cations can be successfully incorporated into the LDH layers in a relative wide range of atomic ratio (Mg/Al = 2–6). The surface area, pore volume and metal composition of the LDHx precursors are collected in Table 1. Evidently, an increase in the Mg/Al atomic ratio of the LDH from 2 to 6 led to a decrease of the LDH surface area and pore volume, indicating that lower Mg/Al ratios can result in a more open LDH structure.

Fig. 2 shows the  $^{27}\text{Al}$  MAS NMR spectra of the LDHx precursors. The signals centered at ca. 9.6 ppm are attributed to six-coordinated (octahedral or  $\text{AlO}_6$ ) aluminum [38]. All spectra of the LDHx precursors are characterized by a single group of  $\text{AlO}_6$  signals, indicating that Al predominantly occupies octahedral sites. This result is in good agreement with the XRD results. Table 1 also shows the surface Mg/Al atomic ratios of the LDHx precursors. Interestingly, there are differences between the Mg/Al ratio in the bulk and at the surface. XPS data suggests a surface enrichment of Al for all LDHx samples.

After calcination at  $500^\circ\text{C}$ , LDOx catalysts were obtained. XRD patterns (Fig. 3) indicate that all catalysts have a MgO-like structure

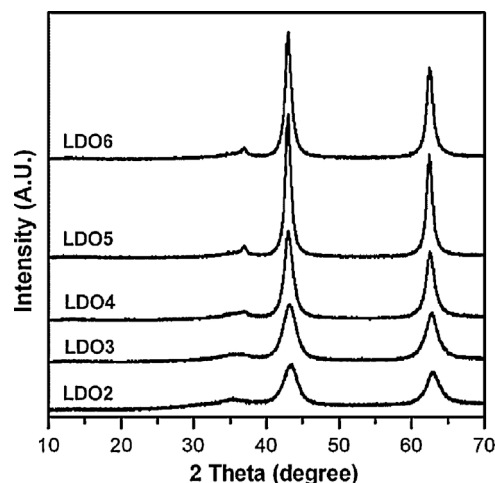


Fig. 3. XRD patterns of the LDOx catalysts.

**Table 1**  
Textural and chemical properties of LDHx precursor.

Sample	$S_{\text{BET}}$ ( $\text{m}^2/\text{g}$ )	Pore volume ( $\text{cm}^3/\text{g}$ )	Mg/Al atomic ratio	
			in bulk <sup>a</sup>	in surface <sup>b</sup>
LDH2	103	0.41	1.99:1.00	1.89:1.00
LDH3	97	0.52	2.95:1.00	2.72:1.00
LDH4	62	0.22	3.69:1.00	3.52:1.00
LDH5	53	0.20	4.60:1.00	4.31:1.00
LDH6	16	0.02	5.66:1.00	5.03:1.00

<sup>a</sup> Determined by ICP-OES.

<sup>b</sup> Evaluated by XPS.

where  $\text{Al}^{3+}$  cation is dissolved in the lattice to form a solid solution [39]. The peak intensities increase with the Mg/Al ratio. These mixed oxides possess higher surface area and pore volume than the LDHx precursors (Table 2). Fig. 4 shows that the pore size distributions varied considerably among the calcined LDOx catalysts, with average pore diameters between 9 and 17 nm. XPS analysis reveals that LDOx catalysts have much lower surface  $\text{Mg}^{2+}$  concentration than the LDHx precursors (Table 2), suggesting that calcination can further promote the migration of  $\text{Al}^{3+}$  from the LDH bulk to the surface of the mixed oxides. Fig. 5 presents the O 1s XP spectra for these LDOx catalysts. Three contributions are distinguished after deconvolution, i.e. at 532.9, 531.5 and 529.8 eV. The higher binding energy (BE) peak at  $\sim 533$  eV is assigned to surface adsorbed  $\text{H}_2\text{O}$ . The BE peak at 531.5 eV is attributed to the surface metal-hydroxide

**Table 2**  
Textural and chemical properties of the LDOx catalysts.

Sample	$S_{\text{BET}}$ ( $\text{m}^2/\text{g}$ )	Pore volume ( $\text{cm}^3/\text{g}$ )	Pore diameter (nm) <sup>a</sup>	Mg/Al molar ratio <sup>b</sup>
LDO2	219	0.52	9.5	1.66:1.00
LDO3	197	0.53	10.8	2.46:1.00
LDO4	178	0.64	14.4	2.89:1.00
LDO5	158	0.65	16.5	3.63:1.00
LDO6	155	0.50	12.9	3.46:1.00

<sup>a</sup> Cylindrical pore diameter (PD);  $\text{PD} = 4000 \times \text{pore volume} / S_{\text{BET}}$ .

<sup>b</sup> Evaluated by XPS.

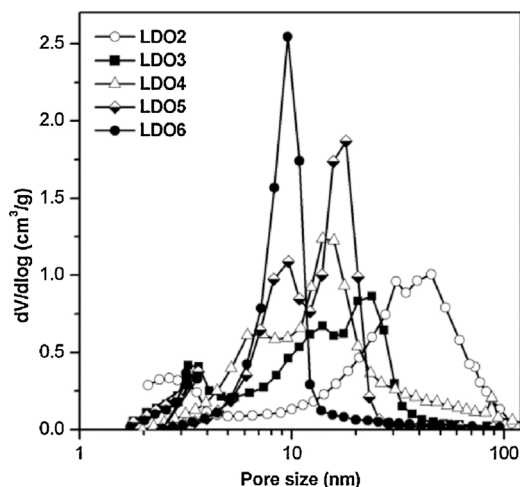


Fig. 4. Pore size distribution of the LDO<sub>x</sub> catalysts from N<sub>2</sub> desorption branch using BJH method.

species. The lower BE peak at 529.8 eV is characteristic for surface O<sup>2-</sup> species [40]. The significant increase in O<sup>2-</sup> character is consistent with the presence of strong Lewis basic sites in the LDO<sub>x</sub> catalysts.

Fig. 6A shows a representative profile of CO<sub>2</sub> release from LDO2 during thermal treatment. Since the LDO2 catalyst was prepared by calcination of LDH2 at 500 °C for 6 h, decomposition of the LDH should be essentially complete [39,41]. However, calcined LDO can absorb water and CO<sub>2</sub> during sample exposure in air, as also evident from the XPS results. Therefore, the LDO<sub>x</sub> catalysts were pre-treated under helium at 500 °C for 1 h before CO<sub>2</sub> adsorption. By CO<sub>2</sub>-TPD measurements (Fig. 6B), CO<sub>2</sub> adsorption volumes and surface basic site densities can be evaluated (Table 3). The range of CO<sub>2</sub> adsorption volumes is between 0.27 and 0.51 mmol/g, with LDO5 and LDO2 showing the lowest and the highest value, respectively. These CO<sub>2</sub> adsorption volumes are similar to that of previously reported MgAl mixed oxides [27,42]. The surface basic site densities increase in the order LDO5 < LDO4 < LDO3 < LDO6 < LDO2. The range of the density of surface basic site is between 1.7 and 2.3 μmol/m<sup>2</sup>, in good agreement with previously reported values for calcined hydrotalcites [27].

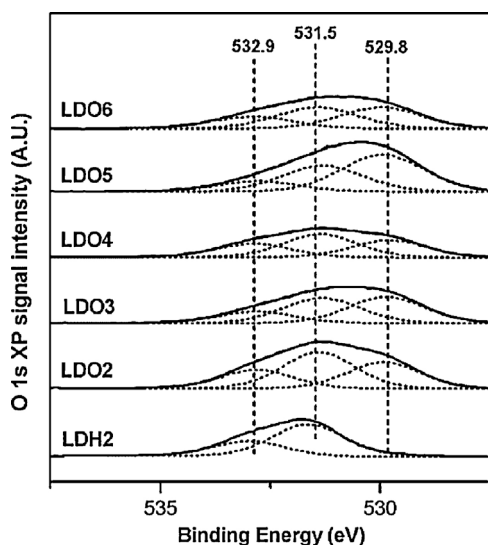


Fig. 5. O 1s XPS spectra for the LDH2 precursor and the LDO<sub>x</sub> catalysts.

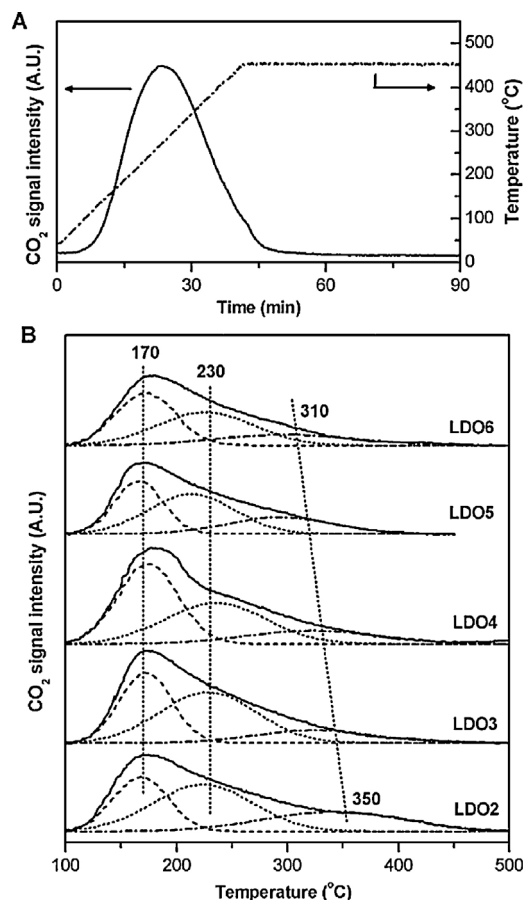


Fig. 6. (A) Release of CO<sub>2</sub> from the LDO2 catalyst during calcination in flowing He with a heating rate 5 °C/min. (B) CO<sub>2</sub>-TPD profiles of the LDO<sub>x</sub> catalysts.

The observed CO<sub>2</sub> desorption peaks can be used to interpret the relationship between the base strength and the calcination temperature. Higher desorption temperature and higher adsorption volume point to higher base strength. In all cases, a broad desorption band is observed between 100 and 500 °C (Fig. 6B), which can be deconvoluted into three main peaks at about 170 °C (weak strength), 230 °C (medium strength) and 300–350 °C (high strength). The medium temperature peak is more intense (38–48% of total area, Table 3), except for LDO4. These medium-strength sites are mainly associated with Mg–O pairs [42]. The low temperature peak can be ascribed to adsorption on surface Brønsted basic site (OH<sup>-</sup> groups). The high temperature peak is attributed to the strong Lewis basic sites of O<sup>2-</sup> anions. Apparently, the base strength distribution of the LDO<sub>x</sub> catalysts varied as a function of the Mg/Al ratio, with LDO2 showing more and stronger high-strength basic sites (27%, 350 °C) than the other LDO<sub>x</sub> containing higher Mg content.

To obtain more insights into the catalyst structure-basicity correlations, we compared the TPSR of pre-adsorbed isopropanol on LDO<sub>x</sub> samples (Fig. 7). It can be clearly seen that the dehydrogenation activity, being related to the catalyst basicity, strongly depends on the Mg/Al ratio (Fig. 7A). The LDO2 catalyst showed significantly higher activity of dehydrogenation at lower temperature (100–200 °C), consistent with the presence of stronger basic sites in the LDO2 sample as indicated by CO<sub>2</sub>-TPD at higher temperature. It is worthwhile noting that propene evolution (Fig. 7B) was similar to acetone evolution (Fig. 7C), although the former showed relatively weaker intensity. This indicates that besides the dehydrogenation occurring over various basic sites, the dehydration can also occur on the acidic Al<sup>3+</sup> sites, consistent with previous results [27,43].

**Table 3**  
Basic properties of the LDOx catalysts.<sup>a</sup>

Sample	CO <sub>2</sub> desorption peaks (area%)			Total CO <sub>2</sub> adsorption (mmol/g)	Basic site density (μmol/m <sup>2</sup> )
	~170 °C	~230 °C	>300 °C		
LDO2	28	45	27	0.51	2.3
LDO3	36	48	16	0.38	1.9
LDO4	45	38	17	0.32	1.8
LDO5	33	45	22	0.27	1.7
LDO6	40	41	19	0.33	2.1

<sup>a</sup> Determined by adsorption and TPD of CO<sub>2</sub>.

The foregoing characterization results demonstrate that the tunability of Mg/Al atomic ratio can be used to fine-tune the structural, textural and chemical properties of the calcined LDHs. The “coprecipitation–calcination” process yields LDOx catalysts with

high surface area and pore volume. The Mg/Al ratio also has an influence on the surface basic site density and alcohol dehydrogenation activity, thus potentially affecting the catalytic performance in glycerol transesterification.

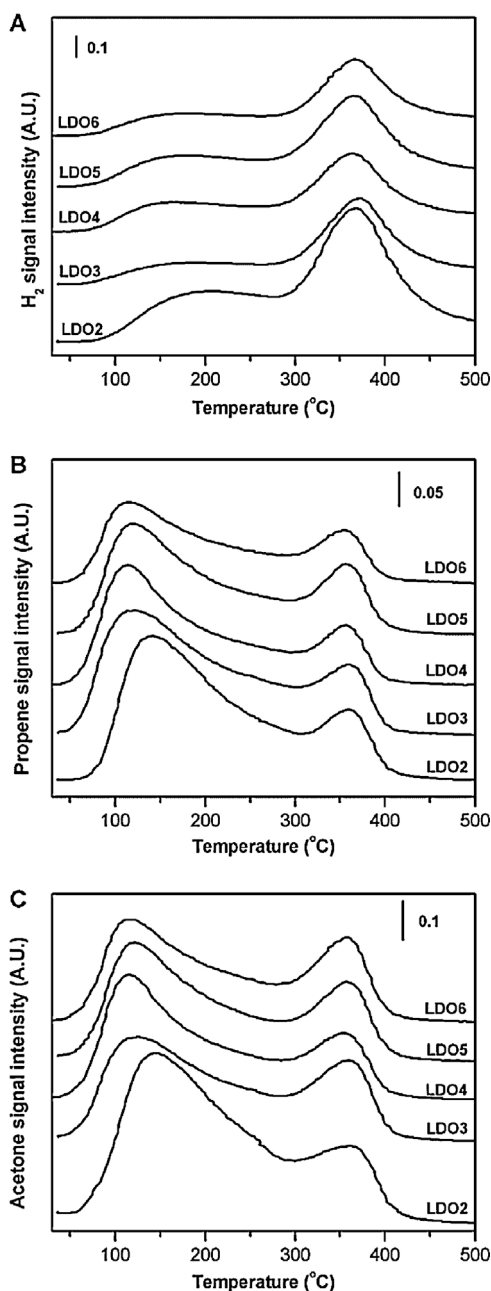


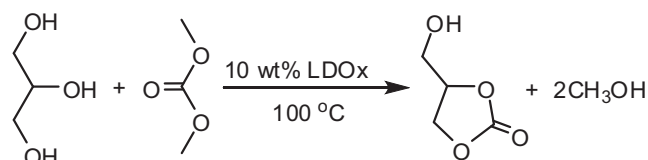
**Fig. 7.** Evolution of H<sub>2</sub> (A), propene (B) and acetone (C) during TPSR of pre-adsorbed isopropanol for the LDOx catalysts.

### 3.2. Catalytic performance

#### 3.2.1. Effect of Mg/Al ratio

The transesterification of glycerol with dimethyl carbonate was chosen as the model reaction to evaluate the catalytic performance of the various LDOx catalysts (Scheme 1). Diethyl carbonate was not chosen as the substrate mainly due to higher reaction temperatures required for its conversion, thus resulting in lower glycerol carbonate selectivity [33–36]. The reaction was initially performed with 10 wt% of LDOx and 3 equiv. of DMC at 100 °C under organic solvent-free conditions.

As shown in Fig. 8, the GLC yield after 2 h reaction differed significantly among the LDOx catalysts. LDO5 gave the lowest yield of GLC (42%), whereas LDO2 achieved the highest yield (56%). The catalytic activity increased in the order LDO5 < LDO4 < LDO3 < LDO6 < LDO2, which is in good agreement with the trend of surface basic site density. The higher activity of LDO2 is also consistent with previously reported results, which showed similar activity trend, i.e. LDO2 > LDO3 > LDO4 [34]. It is noteworthy that all LDOx catalysts gave 100% GLC selectivity. The GLC yield was negligible in the absence of catalyst.



**Scheme 1.** Synthesis of GLC by transesterification of glycerol with DMC.

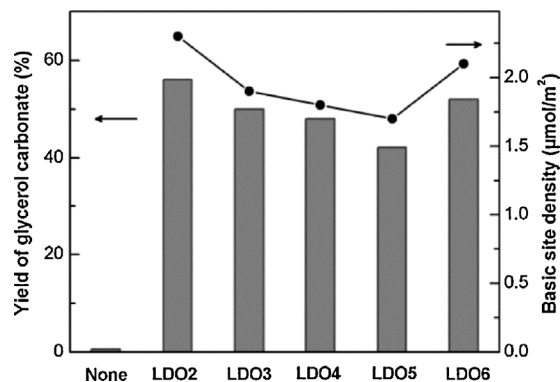


**Fig. 8.** Catalytic performance of the LDOx catalysts for the synthesis of glycerol carbonate. Reaction conditions: 5 mmol glycerol, 10 wt% of LDOx catalyst, 15 mmol DMC, 2 mmol 1,4-butanediol, 100 °C, 2 h.

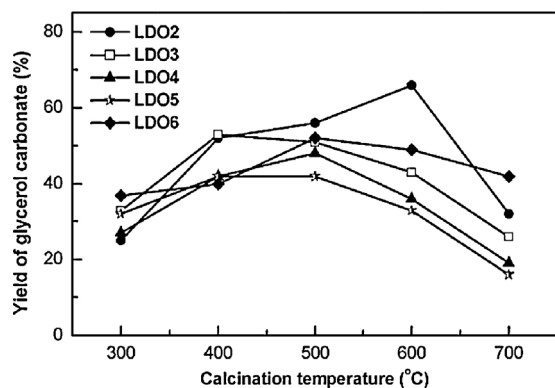


**Fig. 9.** Effect of calcination temperature of the LDO<sub>x</sub> catalysts on the catalytic activity of glycerol transesterification with DMC. Reaction conditions: 5 mmol glycerol, 10 wt% of LDO<sub>x</sub> catalyst, 15 mmol DMC, 2 mmol 1,4-butanediol, 100 °C, 2 h.

Clearly, the good correlation between the catalytic activity and the surface basic site density of LDO<sub>x</sub> catalysts points to the importance of catalyst basicity in the transesterification reaction. It is well known that the basicity of calcined LDH depends not only on the metal composition but also on the calcination temperature [37,40,42]. Therefore, it is possible to further improve the basicity and catalytic activity of LDO<sub>x</sub> catalysts by varying the calcination temperature.

### 3.2.2. Effect of catalyst calcination temperature

To obtain optimum transesterification activity, various LDO<sub>x</sub> catalysts were calcined at different temperatures (300–700 °C) before their use in the reaction. The results are presented in Fig. 9. Evidently, each LDO<sub>x</sub> catalyst has its own optimum calcination temperature. LDO3 showed optimal activity when calcined at 400 °C. LDO4, LDO5 and LDO6 achieved maximum GLC yield after calcined at 500 °C. While 600 °C is the optimum calcination temperature for LDO2 catalyst, the other LDO<sub>x</sub> catalysts show decreased activity after being calcined at 600 °C. Clearly, calcination at 700 °C led to substantial decrease of the activity for all catalysts. In all cases, GLC selectivity is 100% without any byproducts. Among various LDO<sub>x</sub> catalysts and various calcination temperatures, LDO2 calcined at 600 °C exhibited the highest catalytic activity.

It can be speculated that the activity for catalysts calcined at relatively low temperature (300 °C) is mainly related to weak OH<sup>-</sup> sites formed by the decomposition of surface bicarbonate species. Since calcination at 400 °C will only lead to partial decomposition, the activity is attributed to both weakly basic OH<sup>-</sup> sites and the medium-strength Mg–O pair sites. After complete decomposition at higher temperature (500–700 °C), the activity can be ascribed to three kinds of basic sites, i.e. weak OH<sup>-</sup> sites, medium Mg–O pair sites and strong O<sup>2-</sup> sites. For the activity decrease of LDO<sub>x</sub> catalysts at high calcination temperature, it is reasonable to state that the Lewis acidic nature of Al<sup>3+</sup> cations may suppress basicity. This speculation is supported by the fact that the surface Al<sup>3+</sup> concentration increased with calcination temperature, and the CO<sub>2</sub> adsorption volume was lowered for LDO2 upon calcination at 700 °C (Fig. 10). In the case of the optimum LDO2 catalyst, the basicity is significantly improved, probably due to the presence of a large amount of weak-strength OH<sup>-</sup> sites and medium-strength Mg–O basic sites and lack of Lewis acidic sites of Al<sup>3+</sup> when calcined at 600 °C.

### 3.2.3. Influence of reaction conditions

The reaction conditions were further optimized for the LDO2 (@600 °C) catalyst. Fig. 11A shows the effect of reaction temperature. The GLC yield was increased with reaction temperature up to 100 °C and, thereafter, there was a significant decrease in yield.

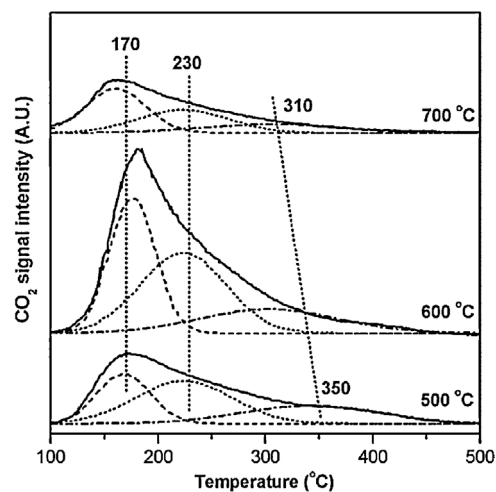


**Fig. 10.** CO<sub>2</sub>-TPD profiles of the LDO2 samples calcined at different temperatures.

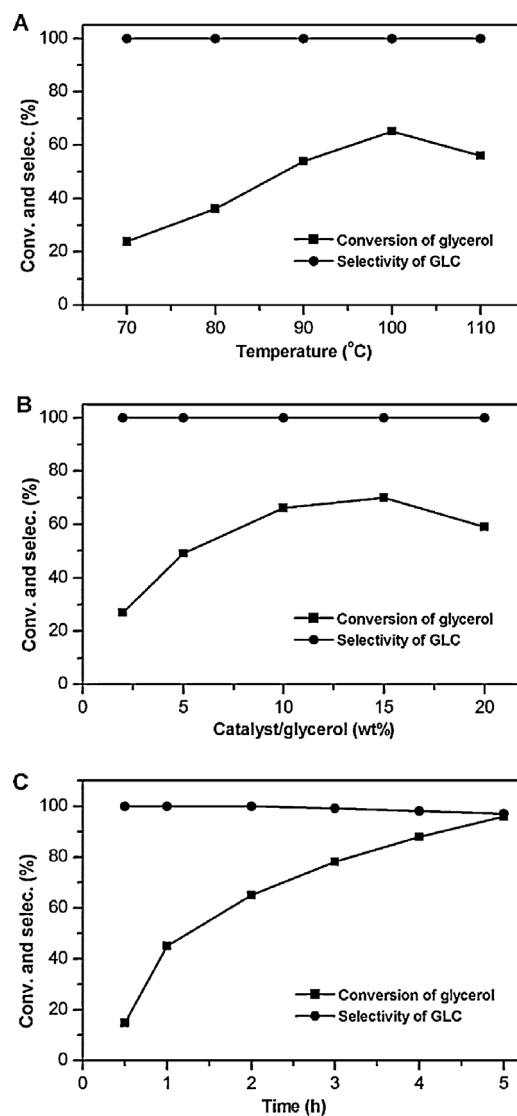


**Fig. 11.** Effect of reaction temperature (A), catalyst amount (B) and reaction time (C) on catalytic performance of LDO2 (@600 °C) catalyst. Typical reaction conditions: 5 mmol glycerol, 10 wt% of LDO2, 15 mmol DMC, 2 mmol 1,4-butanediol, 100 °C, 2 h.

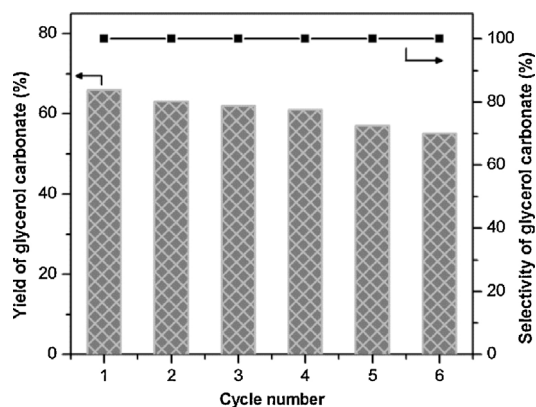


**Fig. 12.** Reusability of LDO2 (@600 °C) catalyst. Reaction conditions: 5 mmol glycerol, 15 mmol DMC, 2 mmol 1,4-butanediol, 100 °C, 2 h; for the first cycle, 10 wt% of LDO2 catalyst was added.

The LDO2 catalyst showed maximum activity at a reaction temperature of 100 °C. The decreased GLC yield (with 100% selectivity) at high temperature suggests that side-reactions (dehydrogenation and condensation) by the byproduct methanol may occur on the basic sites. Fig. 11B presents the influence of the catalyst amount on transesterification reaction. Surprisingly, the GLC yield was not increased when the amount of catalyst was increased. Compared to 10 wt% of catalyst, the activity was even lower when 20 wt% of catalyst was used. When 15 wt% of catalyst was used the GLC yield was similar. This is mainly due to the increased resistance of mass transfer in the solid catalyst-glycerol-DMC triphase system, because catalyst aggregation was clearly observed when catalyst amount increased to more than 10 wt%.

The optimum reaction temperature and catalyst amount were determined to be 100 °C and 10 wt%, respectively. Under these conditions, the effect of reaction time was also investigated and the results are shown in Fig. 11C. Clearly, the transesterification reaction has no apparent induction period. The reaction achieved 96% conversion of glycerol after 5 h but with a slight decrease in GLC selectivity (97%). Glycerol dicarbonate was identified to be the only by-product, which is generally reported as the main by-product for GLC synthesis by transesterification of glycerol with alkyl carbonates and the selectivity can reach up to 30–80% by other calcined or rehydrated LDH catalysts [33–36]. The decrease in GLC selectivity is indicative of some deactivation of the LDO2 catalyst and could be attributed to a strong adsorption of side products on the basic sites during the reaction.

### 3.2.4. Stability of LDO2 catalyst

In order to determine stability of the LDO2 catalyst, the spent catalyst was recycled in the glycerol transesterification reaction. The results are presented in Fig. 12. The solid catalyst could be readily separated from the reaction mixture by centrifugation and used in next cycle after washing and drying. To our delight, LDO2 could be recycled and reused at least five times without significant loss of activity and selectivity, and the GLC selectivity retained 100%, even after the repetitive use. Subsequently, the fifth recycled catalyst was tested by XRD and XPS. XRD results confirm retention of the original MgO-like structure (Fig. 13A). XPS evidences a different surface metal composition for the recycled catalyst with Mg/Al=1.58:1.00. Compared to the fresh catalyst (Mg/Al=1.63:1.00), an increase in surface Al concentration was observed, indicating that more Al<sup>3+</sup> in the bulk phase gradually transferred to the surface. Fig. 13B shows the O 1s XP spectra for the fresh and fifth recycled LDO2 catalyst. The decrease in O<sup>2-</sup> character (529.8 eV) for the reused catalyst supports the speculation that side products may adsorb on the strong basic sites during

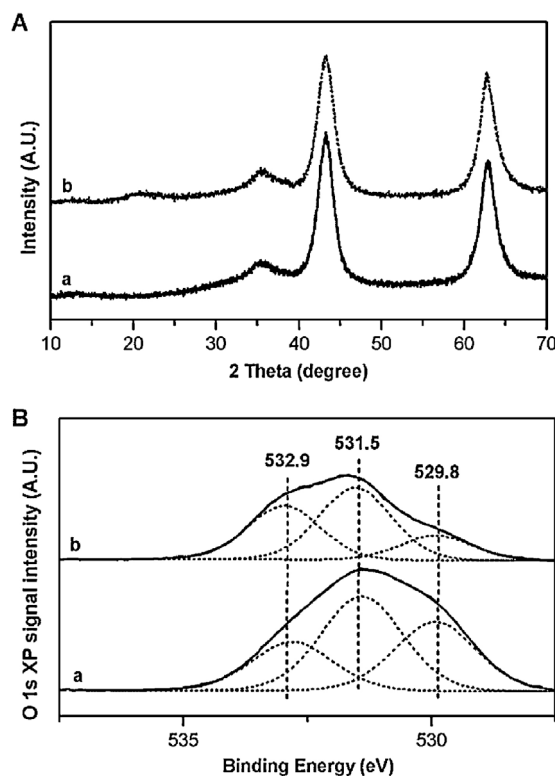


**Fig. 13.** XRD patterns (A) and XP spectra (B) of the fresh (a) and fifth recycled (b) LDO2 (@600 °C) catalyst.

the reaction. From the structural information of the recycled LDO2 catalyst, the reconstruction of the layered LDH2 structure by the “memory effect” can be excluded. This is mainly due to the anhydrous conditions we applied during reactions and catalyst recovery processes. Significantly, the optimum LDO2 catalyst showed higher stability than previously reported rehydrated LDH catalysts in the transesterification of glycerol to GLC [33,34].

### 3.2.5. Activity comparison of the LDO2 catalyst with other reference catalysts

Since most previous studies use quite different reaction conditions, it is difficult to directly compare the activity of our LDO2 catalyst with previously reported base catalysts. Therefore, we prepared and compared several representative reference catalysts under our reaction conditions and the results are shown in Table 4. Evidently, the LDH2 precursor showed much lower activity than LDO2 catalyst, mainly due to the presence of only weak-strength basic sites in the uncalcined sample. LDO2 outperforms MgO under identical conditions, further confirming the beneficial effect of the optimum ratio of Mg/Al=2 on catalyst basicity and activity. CaO and

**Table 4**

Comparison of the catalytic activity of LDO2 with other reference catalysts for the synthesis of glycerol carbonate.<sup>a</sup>

Catalyst	Time (h)	GLC yield (%)	GLC selectivity (%)
LDO2 <sup>b</sup>	2	66	100
LDH2	2	24	100
MgO <sup>b</sup>	2	50	100
CaO <sup>c</sup>	1	79	81
NaOH <sup>d</sup>	1	70	70

<sup>a</sup> Reaction conditions: 5 mmol glycerol, 15 mmol DMC, 2 mmol 1,4-butanediol, and 10 wt% of catalyst, 100 °C.

<sup>b</sup> Calcined at 600 °C.

<sup>c</sup> Calcined at 900 °C.

<sup>d</sup> 2 wt% of catalyst was used.

NaOH exhibited much higher activity but with significantly lower GLC selectivity, in agreement with previously reported results [13,44]. Moreover, CaO cannot be reused unless regenerated at high temperature (900 °C) [13]. Based on the above results, we can conclude that the LDO2 calcined at 600 °C is a stable and practical catalyst for glycerol carbonate synthesis by glycerol transesterification with dimethyl carbonate under solvent-free conditions.

#### 4. Conclusions

In summary, we have shown that the Mg/Al atomic ratio of hydrotalcite-like LDHs strongly affects the basicity and catalytic activity of calcined LDOx mixed oxides for the transesterification of glycerol with dimethyl carbonate to glycerol carbonate. The basicity of LDOx can be fine-tuned by simple adjustment of the Mg/Al ratio and the calcination temperature. The catalytic performance of the LDOx catalysts depends on the Mg/Al ratio, the surface basicity and the reaction conditions. A good correlation between catalytic activity and surface basic site density of the LDOx catalysts has been established. LDO2 catalyst calcined at 600 °C shows maximum activity, which has been attributed to the beneficial effect of the optimum ratio of Mg/Al=2 on enhancement of catalyst basicity. The optimum LDO2 catalyst can be readily recovered and reused with no significant loss of performance. These findings provide insights into the structure–basicity–activity relationship of the calcined hydrotalcite catalysts, and make it possible to design more efficient solid base catalysts for various base-catalyzed reactions.

#### Acknowledgments

This research was financially supported by Programme Strategic scientific Alliances between the Netherlands and China (Grant No. 2008DFB5-130).

#### References

- [1] M. Pagliaro, R. Ciriminna, H. Kimura, M. Rossi, C.D. Pina, *Angew. Chem. Int. Ed.* 46 (2007) 4434–4440.
- [2] C.-H. Zhou, J.N. Beltramini, Y.-X. Fan, G.Q. Lu, *Chem. Soc. Rev.* 37 (2008) 527–549.
- [3] A. Behr, J. Eilting, K. Irawadi, J. Leschinski, F. Lindner, *Green Chem.* 10 (2008) 13–30.
- [4] J.R. Ochoa-Gómez, O. Gómez-Jiménez-Aberasturi, C. Ramírez-López, M. Belsué, *Org. Process Res. Dev.* 16 (2012) 389–399.
- [5] M.O. Sonnat, S. Amigoni, E.P.T. de Givenchy, T. Darmanin, O. Choulet, F. Guitard, *Green Chem.* 15 (2013) 283–306.
- [6] M. Aresta, A. Dibenedetto, F. Nocito, C. Pastore, *J. Mol. Catal. A: Chem.* 257 (2006) 149–153.
- [7] J. George, Y. Patel, S.M. Pillai, P. Munshi, *J. Mol. Catal. A: Chem.* 304 (2009) 1–7.
- [8] C. Vieville, J.W. Yoo, S. Pelet, Z. Mouloungui, *Catal. Lett.* 56 (1998) 245–247.
- [9] M. Aresta, A. Dibenedetto, F. Nocito, C. Ferragina, *J. Catal.* 268 (2009) 106–114.
- [10] M.J. Climent, A. Corma, P.D. Frutos, S. Iborra, M. Noy, A. Vely, P. Concepción, *J. Catal.* 269 (2010) 140–149.
- [11] C. Hammond, J.A. Lopez-Sanchez, M.H.A. Rahim, N. Dimitratos, R.L. Jenkins, A.F. Carley, Q. He, C.J. Kiely, D.W. Knight, G.J. Hutchings, *Dalton Trans.* 40 (2011) 3927–3937.
- [12] S.-i. Fujita, Y. Yamanishi, M. Arai, *J. Catal.* 297 (2013) 137–141.
- [13] J.R. Ochoa-Gómez, O. Gómez-Jiménez-Aberasturi, B. Maestro-Madurga, A. Pesquera-Rodríguez, C. Ramírez-López, L. Lorenzo-Ibarreta, J. Torrecilla-Soria, M.C. Villarán-Velasco, *Appl. Catal. A: Gen.* 366 (2009) 315–324.
- [14] H. Hattori, *Chem. Rev.* 95 (1995) 537–558.
- [15] G. Busca, *Chem. Rev.* 110 (2010) 2217–2249.
- [16] F. Cavani, F. Trifiró, A. Vaccari, *Catal. Today* 11 (1991) 173–301.
- [17] D. Tichit, B. Coq, *Cattech* 7 (2003) 206–217.
- [18] D.P. Debecker, E.M. Gaigneaux, G. Busca, *Chem. Eur. J.* 15 (2009) 3920–3935.
- [19] B.F. Sels, D.E. De Vos, P.A. Jacobs, *Catal. Rev. Sci. Eng.* 43 (2001) 443–488.
- [20] F. Figueras, *Top. Catal.* 29 (2004) 189–196.
- [21] D. Tichit, C. Gérardin, R. Durand, B. Coq, *Top. Catal.* 39 (2006) 89–96.
- [22] Z.P. Xu, J. Zhang, M.O. Adebajo, H. Zhang, C. Zhou, *Appl. Clay Sci.* 53 (2011) 139–150.
- [23] P. Liu, H. Wang, Z. Feng, P. Ying, C. Li, *J. Catal.* 256 (2008) 345–348.
- [24] P. Liu, C. Wang, C. Li, *J. Catal.* 262 (2009) 159–168.
- [25] P. Liu, Y. Guan, R.A. van Santen, C. Li, E.J.M. Hensen, *Chem. Commun.* 47 (2011) 11540–11542.
- [26] P. Liu, C. Li, E.J.M. Hensen, *Chem. Eur. J.* 18 (2012) 12122–12129.
- [27] A.L. Mckenzie, C.T. Fishel, R.J. Davis, *J. Catal.* 138 (1992) 547–561.
- [28] A. Corma, V. Fornés, F. Rey, *J. Catal.* 148 (1994) 205–212.
- [29] J.C.A.A. Roelofs, D.J. Lensveld, A.J. van Dillen, K.P. de Jong, *J. Catal.* 203 (2001) 184–191.
- [30] F. Winter, X. Xia, B.P.C. Hereijgers, J.H. Bitter, A.J. van Dillen, M. Muhler, K.P. de Jong, *J. Phys. Chem. B* 110 (2006) 9211–9218.
- [31] A. Takagaki, K. Iwatani, S. Nishimura, K. Ebitani, *Green Chem.* 12 (2010) 578–581.
- [32] A. Kumar, K. Iwatani, S. Nishimura, A. Takagaki, K. Ebitani, *Catal. Today* 185 (2012) 241–246.
- [33] M.G. Álvarez, A.M. Segarra, S. Contreras, J.E. Sueiras, F. Medina, F. Figueras, *Chem. Eng. J.* 161 (2010) 340–345.
- [34] M.G. Álvarez, R.J. Chimentao, F. Figueras, F. Medina, *Appl. Clay Sci.* 58 (2012) 16–24.
- [35] M.G. Álvarez, M. Pliskova, A.M. Segarra, F. Medina, F. Figueras, *Appl. Catal. B: Environ.* 113–114 (2012) 212–220.
- [36] M.G. Álvarez, A.M. Frey, J.H. Bitter, A.M. Segarra, K.P. de Jong, F. Medina, *Appl. Catal. B: Environ.* 134–135 (2013) 231–237.
- [37] M. Malyaadri, K. Jagadeeswaraiyah, P.S.S. Prasad, N. Lingaiah, *Appl. Catal. A: Gen.* 401 (2011) 153–157.
- [38] A. Vyalikh, F.R. Costa, U. Wangenknecht, G. Heinrich, D. Massiot, U. Scheler, *J. Phys. Chem. C* 113 (2009) 21308–21313.
- [39] F. Millange, R.I. Walton, D. O'Hare, *J. Mater. Chem.* 10 (2000) 1713–1720.
- [40] D.G. Cantrell, L.J. Gillie, A.F. Lee, K. Wilson, *Appl. Catal. A: Gen.* 287 (2005) 183–190.
- [41] P. Liu, M. Derchi, E.J.M. Hensen, *Appl. Catal. B: Environ.* (2013), <http://dx.doi.org/10.1016/j.apcatb.2013.07.010>.
- [42] J.I.D. Cosimo, V.K. Díez, M. Xu, E. Iglesia, C.R. Apesteguía, *J. Catal.* 178 (1998) 499–510.
- [43] C.T. Fishel, R.J. Davis, *Langmuir* 10 (1994) 159–165.
- [44] R. Bai, Y. Wang, S. Wang, F. Mei, T. Li, G. Li, *Fuel Process. Technol.* 106 (2013) 209–214.